

Microscale surface catalysis for silicon MEMS monopropellant chemical microthruster

Y. Feng^{a,b}, J.L. Xu^a

^a Micro Energy System Laboratory, Guangzhou Institute of Energy Conversion, Chinese Academy of Sciences, Nengyuan Road, Wushan, Guangzhou, 510640, P.R.China

^b Graduate School of Chinese Academy of Sciences, Beijing, 100039, P.R.China
E-mail: xujl@ms.giec.ac.cn

Abstract

Precise attitude control and orbit manoeuvring are important for the micro/nanosatellites. Microthruster can fulfill such function thus it has been received great attention in recent years. In this paper, a silicon MEMS based microthruster was developed, which consists of an inlet liquid plenum, nine parallel rectangular microchannels and a planar convergent-divergent nozzle. A high speed camera system incorporating a microscope was used to perform the flow visualization in the microthruster. It is observed that the hydrogen peroxide decomposition and two-phase flow display the strong periodic behavior. A full cycle can be divided into three substages: a quick liquid refilling stage, a liquid decomposition stage and a two-phase flow stage. In the two-phase flow stage, it is observed that the whole microchannel length is covered by a successive of liquid droplets separating a set of bubble slugs.

Keywords: microthruster, hydrogen peroxide, two-phase flow, micro reactor

1. Introduction

In recent years, great attention was paid on the micro/nanosatellite with the weight down to 10-100kg. In such a system miniature thrust force is necessary to be provided for attitude control and orbit manoeuvring. The fast development MEMS technology satisfy the microthruster fabrication requirement. Cold gas, solid propellant[1], hydrogen peroxide[2] and water[3] are the possible working media. Microthruster with water in a micro chamber heated by the internal heating resistor is an energy consuming system. Compared with the water microthruster, a hydrogen peroxide microthruster is an energy saving one.

Even though the hydrogen peroxide microthruster has been demonstrated for the military or space applications from the working principle point of view, little is known on the complicated liquid decomposition and two-phase

flow in microthrusters. One key issue is the critical residence time of the microreactor. Lacking a sound theory to proceed the suitable microreactor length, the empirical catalyst lengths reported in literature for macroscale thrusters and scaling these predictions down to MEMS scale yields the microreactor length of 1.7-2.0mm. Such estimation is questionable due to neglecting the microscale effects such as surface tension force.

2. Experiment setup

Fig.1 shows the designed microthruster. The etched silicon chip is bonded with a pyrex glass through which the transient hydrogen peroxide decomposition and two-phase flow can be easily observed. The nine microchannels have the length of 6.0mm, covering the total width of 1120 μm . Each microchannel has the width of 80 μm and depth of 120 μm . The fabrication is a standard microfabrication process in the clean

room and the catalyst thin platinum film with the thickness of 150 nm was deposited on the etched silicon surface by sputtering.

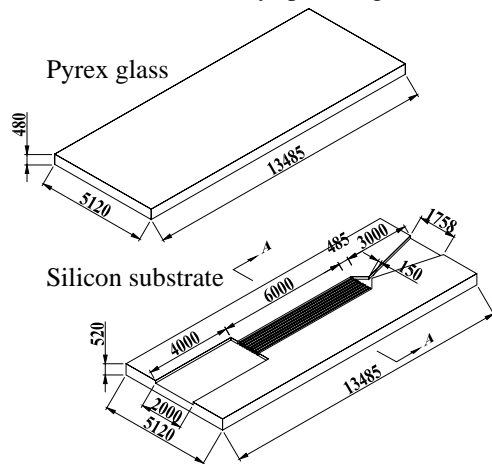


Fig.1 Schematic diagram of the microthruster

Fig.2 shows the experimental setup for the microthruster measurement. The hydrogen peroxide liquid in the reservoir tank is pressurized by the nitrogen gas and flows successively through the soft plastic capillary tube, a two micron filter and enters the microthruster. In order to quantify the level of decomposition in the catalyzed microthruster, the liquid phase components of the exit flow were collected and analyzed for hydrogen peroxide concentration. Liquids are observed in the planar converging-diverging nozzle. Later it is shown that the not complete decomposition of hydrogen peroxide is caused by the liquid droplet formation in microchannels.

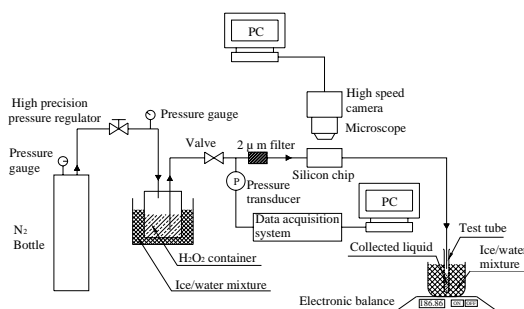


Fig.2 Schematic diagram of experimental setup

The microthruster discharges the mixture of gas and liquid at the exit environment pressure. The pressure drop across the microthruster is measured by a high precision Senex pressure drop transducer with the

uncertainty of 0.1%. The data was collected by A HP data acquisition system.

A high speed camera system incorporating a microscope was used to observe the hydrogen peroxide decomposition and two-phase flow in microthruster. The recording rates selected based on how fast the transient flow is. For the present applications, the recording rates are selected as 125 images per second.

3.Results and discussion

It is found that isolated bubble flow and bubble slug flow are the two major flow patterns. The isolated bubbles are identified as the blurred images at the hydrogen peroxide decomposition stage. In the bubble slug flow stage, a set of liquid droplets are formed to separate a successive of bubble slugs. Once the isolated bubble densities are increased to a critical value leading to the shortened distance between the neighboring bubbles, the transition from the isolated bubbles to the bubble slug flow takes place.

Figs.3-4 shows the transient liquid decomposition and bubble slug flow in single microchannel for microchannel 9 which is the side channel, for the hydrogen peroxide concentration of 60% and pressure drop of 15kpa. The initial time $t = 0$ is defined for each channel independently due to the isochronous transient process among different channels. In microchannel 9, the fresh hydrogen peroxide liquid covers the whole channel at $t = 0$ (see Fig.3). The hydrogen peroxide decomposition process sustains in the time from 256ms to 600ms, which was indicated by the blurred images. The coalescence of the isolated bubbles are to form the bubble slugs in downstream part of the microchannel for the time of 728ms to 1048ms. There are maximum numbers of liquid droplets at the first critical time at $t = 1048ms$. The liquid droplets are marked from A to J at $t = 1048ms$.

The bubble slug flow starts from 1048ms. The

liquid droplet trajectories can be easily identified by a set of transient images versus time. Flow reversal was observed for liquid droplets J and I, indicated by the decreased displacements of liquid droplets versus time. Because the liquid droplets are continuously out of microchannels, for instance, the liquid droplets A, B and C disappear in the microchannel 9 at

$t = 1208ms$, $t = 1648ms$ and $t = 1888ms$ respectively, the bubble slug lengths are increased while the number of liquid droplets is decreased. The fluid is quickly flushed out of the microchannel around at 2824ms. A new cycle begins with fresh liquid refilling the microchannels (see Fig.3, $t = 2840ms$)

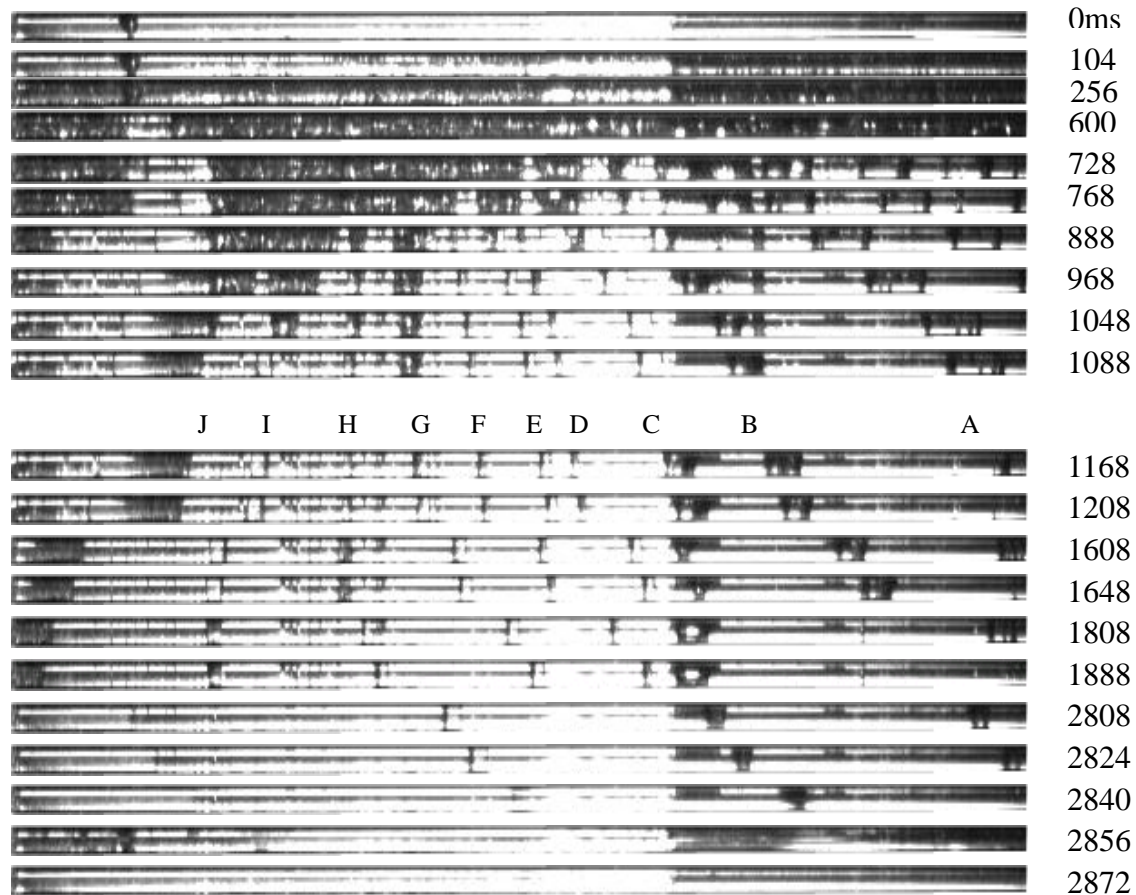


Fig.3. Hydrogen peroxide decomposition process in microchannel 9 at 60% reservoir hydrogen peroxide concentration and 15kpa pressure drop

Fig.4 illustrates the liquid droplet displacements and bubble slug lengths. It is noted that the initial time at $t = 0$ in Fig.4 actually starts from the bubble slug flow stage, not including the hydrogen peroxide decomposition process. $t = 0$ is also the first critical state at which there are the maximum number of liquid droplets. The second critical time is marked as t_a at which three or four liquid droplets existed in channels. The less number of liquid droplets are quickly flushed out

of channels following the second critical time.

One may concern another issue that how fast the liquid droplet traveling velocities are. The surface tension force effect is strong in microscale such as encountered in the present paper. In Fig.4 there are ten liquid droplets in the microchannel at $t = 0$, the applied pressure drop on each liquid droplet is only 1.5kpa. Thus the excess net pressure computed from the applied pressure drop on each liquid droplet subtracting the pressure drop due to the surface tension effect is small, leading to the slow

moving velocity before the second critical time. However, the excess net pressure on a single liquid droplet becomes quite large with less liquid droplets such as three in the microchannel, leading to the acceleration of the liquid droplets, which can be identified following t_a in Fig.4.

The initial bubble slug lengths (bubble slug lengths at $t = 0$ in Fig.4) are very important to select a suitable microreactor length. The bubble slug lengths are in the range of 0.5mm to 1.0mm for the hydrogen peroxide concentration from 60% to 90%. Such measured bubble slug lengths are almost one third of the critical reactor length of 1.7-2.0mm given by Hitt [2]. One can expect the annular flow pattern in microchannels if the microreactor length is identical of the initial bubble slug length. No liquid droplets exist for the annular flow pattern, leading to the possible complete hydrogen peroxide decomposition.

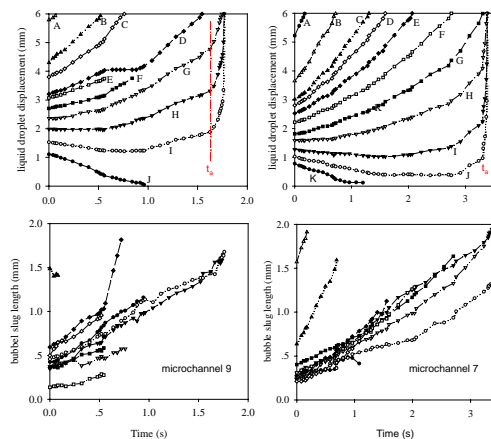


Fig.4 Liquid droplet displacement and bubble slug length versus time for 60% concentration, 15kpa of pressure drop

Either bubble slug flow or annular flow exists in microchannels once the isolated bubbles coalesce. Little is known on such flow pattern transition in microscale, especially under the condition of catalyzed chemical reaction. A lot of parameters, such as the microchannel size, hydrogen peroxide concentration and pressure drop, affect the formation of the bubble slug flow and annular

flow. The experimental decided bubble slug lengths in the present study are helpful to provide a guideline for selection of the microchannel length, preventing the liquid droplet formation. Further studies are recommended on the chip temperature effect on the liquid droplets and bubble slug length distributions in microchannels. Flow pattern theory or empirical correlations are also expected in microscale.

4. Conclusions

We performed the high speed flow visualization on the complicated liquid decomposition and two-phase flow in microchannel-based microthruster. It is observed that the transient process displays the strong cycle behavior. A full cycle consists of the quick liquid refilling stage, a liquid decomposition stage, and a bubble slug flow stage. The initially bubble slugs have the lengths in the range of 0.5 to 1.0mm in the present data range, which are much shorter than those predicted by the classical theory in macroscale

Acknowledgements

The present work is supported by the International Cooperation Project Funding from Chinese Academy of Science and Natural Science Foundation of China with the contract number of 50476088

References

1. Zhang K L, Chou S K, Ang S S, 2004, MEMS-based solid propellant microthruster design, simulation, fabrication and testing, J. of Microelectromechanical Systems, 13(2), 165-175
2. Hitt D.L., Zakrzewski C.M., and Thomas M.A., 2001, MEMS-based satellite micropropulsion via catalyzed hydrogen peroxide decomposition, Smart Mater. Struct., 10, 1163-1175
3. Maurya D. K., Das S and Lahiri S.K., 2005, Silicon MEMS vaporizing liquid microthruster with internal microheater, J. of Micromechanics and Microengineering, 15, 966-970